Influence of free carriers on exciton ground states in quantum wells

A.A. Klochikhin [a,b], V.P. Kochereshko [a,c,*], S. Tatarenko [d]

[a] Ioffe Physical Technical Institute, 194021 St. Petersburg, Russia
[b] Nuclear Physics Institute, 350000 St. Petersburg, Russia
[c] Spin Optics Laboratory, St. Petersburg State University, 198904 St. Petersburg, Russia
[d] CEA-CNRS Group "Nanophysique et Semiconducteurs", Institut Néel, CNRS and Universite Joseph Fourier, 25 Avenue des Martyrs, 38042 Grenoble, France

ARTICLE INFO

ABSTRACT

The influence of free carriers on the ground state of the exciton at zero magnetic field in a quasi-two-dimensional quantum well that contains a gas of free electrons is considered in the framework of the random phase approximation. The effects of the exciton–charge-density interaction and the inelastic scattering processes due to the electron–electron exchange interaction are taken into account. The effect of phase-space filling is considered using an approximate approach. The results of the calculation are compared with the experimental data.

© 2014 Elsevier B.V. All rights reserved.

1. Introduction

The presence of free electrons in quasi-two-dimensional semiconductor structures strongly alters their physical characteristics. At low and intermediate electron concentrations, the Coulomb interaction between the electrons and the holes leads to formation of the bound exciton state. In addition, starting from very low concentrations of free electrons in the quantum well, a bound trion (negatively charged exciton) state [11–14] is observed in experiments [6–10]. At high concentrations the free electrons causes a static screening of the electron–hole Coulomb potential. The screening as well as the filling of phase-space up to the Fermi energy leads to a strong decrease of the exciton binding energy. At some concentration of free electrons the bound states disappear and the so-called Mahan exciton can be expected. Considerable attention has been paid in the literature to experimental and theoretical investigations of the 2D-systems at high concentration of free carriers. The theory of this phenomenon was developed in Ref. [1] for the 3D crystal and in Refs. [2–5] for 2D systems. Experimental data [6–10] give evidence that, within a relatively narrow interval of free electron concentrations below the metallic phase, the optical absorption band associated with the bound exciton shifts and broadens, and its oscillator strength decreases as carrier concentration is increased. The dependence of these characteristics on the electron concentration allows one to relate these processes with exciton–electron interactions. The observed

broadening of the exciton line [6–9] clearly shows that not only static screening but also inelastic dynamical processes should be considered for the explanation of the exciton spectrum.

The exciton created by a photon has almost zero wave-vector. Further interaction of the exciton with free electrons followed by scattering of a conduction electron near the Fermi level with $p \approx p_F$ creates a conduction electron–conduction hole pair. This pair has an arbitrary wave-vector of the center of mass motion $\mathbf{q}$ and an energy $\hbar^2 q^2/2m + \hbar^2 \mathbf{pq}/m$ which is the difference between the conduction electron's energy in the final and initial states ($\hbar^2(\mathbf{p+q})^2/2m$ and $\hbar^2 \mathbf{p}^2/m$, respectively).

The threshold energy of this excitation at $q=0$ and temperature $T=0$ K is zero. Therefore, the lower boundary of the continuum spectrum of the combined excitation consisting of the free exciton plus an electron–conduction hole pair coincides with the energy of the free exciton. As a consequence, this inelastic scattering process results in a homogeneously broadened absorption spectrum with its maximum shifted toward high energies with increasing free electron concentration.

The mechanism responsible for the creation of an electron (above Fermi surface)–hole (below Fermi surface) pair can be either the Coulomb interaction or the exchange interaction between the electron bound in the exciton and the free electrons.

For the negatively charged trion, which has two bound electrons coupled in a spin singlet state, the Coulomb interaction seems to be the only important mechanism of interaction with free electrons [15]. In the case of the electrically neutral exciton the strong cancellation of the electron and valence hole self-energy corrections and vertex correction decreases the role of the Coulomb interactions in the scattering processes. This means that the exchange interaction between the electron belonging to the

exciton and a free electron should be considered as the most probable reason for the broadening of the exciton absorption band.

We consider in detail the behavior of the bound exciton absorption band as a function of free electron concentration in a quantum well doped by electrons at low and intermediate concentrations, and we extrapolate the results up to the concentration at which the bound exciton state disappears.

We will show in this paper that a second order exchange process strongly influences the bound exciton state and the optical spectra of the doped quantum wells, in addition to the nearly rigid band gap renormalization produced by the first order exchange interaction. The second order process broadens the exciton absorption band and shifts the energy of its maximum.

The paper is organized as follows. In Section 2 we formulate the exciton equation in a quasi-two-dimensional quantum well containing free electrons using the known results for the 3D case. We take into account in this section the static screening of the Coulomb interaction and the effect of phase-space filling. Section 3 is devoted to the exchange interaction between the electron constituting the exciton and the free electrons. In Section 4 we describe the calculation of the absorption coefficient as a function of the free electron concentration and give a comparison with experimental data.

2. Exciton in a quantum well

We consider only temperature $T \to 0$ K assuming that $k_B T$ is much less than the Fermi energy. Despite the reduced dimensionality there exists a deep analogy with the 3D Fermi systems in the methods of calculation of multi-particle effects.

The exciton equation can be formulated by summing the ladder diagrams for the exciton Green function similarly to the procedure described by Mahan [1]. Accepting this paper as a guide we present the exciton equation in a quantum well with finite concentration of free electrons as

$$-\frac{\nabla^2}{2\mu}\psi_\lambda(\overrightarrow{\rho}) + \int d^2\rho' V^{2D}(\rho')K(\overrightarrow{\rho}-\overrightarrow{\rho'})\psi(\overrightarrow{\rho}) = E_\lambda \psi_\lambda(\overrightarrow{\rho}), \qquad (1)$$

where $\mu = m_e m_h/(m_e+m_h)$ is the reduced mass of the electron and valence hole, $\overrightarrow{\rho}$ is the two-dimensional radius-vector between the electron and hole positions in the exciton. $V^{2D}(\overrightarrow{\rho})$ is the quasi-two-dimensional Coulomb potential at zero temperature (in the calculation of which the static screening should be taken into account), and

$$K(\rho) = -\frac{1}{(2\pi)^2}\int d^2\hat{q}\, e^{i\hat{\mathbf{q}}\overrightarrow{\rho}}(1-\Theta(\hat{p}_F-\hat{q})), \qquad (2)$$

where $\hat{p}_F$ is the Fermi wave vector, $\Theta(\hat{p}_F-\hat{q})$ is the step-like theta-function, and $(1-\Theta(\hat{p}_F-\hat{q}))$ is the Fermi distribution function at zero temperature restricting the integral region in two-dimensional reciprocal space to $\hat{q} \leq \hat{p}_F$. We present $K(\rho)$ as two items

$$K(\rho) = -\delta(\rho) + \frac{1}{(2\pi)^2}\int d^2\hat{q}\, e^{i\hat{\mathbf{q}}\overrightarrow{\rho}}\Theta(\hat{p}_F-\hat{q}). \qquad (3)$$

After substitution of Eq. (3) into Eq. (1) we obtain two items for the exciton potential energy. The first item is an attractive potential $V^{2D}(\overrightarrow{\rho})$ and the second is a repulsive term that arises due to phase-space filling

$$\delta V^{2D}(\rho) = \frac{1}{(2\pi)^2}\int d^2\hat{q} \int d^2\overrightarrow{\rho'}\, V^{2D}(\rho')e^{i\hat{\mathbf{q}}(\overrightarrow{\rho}-\overrightarrow{\rho'})}\Theta(\hat{p}_F-\hat{q}) \qquad (4)$$

The matrix element of this equation responsible for the correction

to the exciton energy is

$$\int d^2\overrightarrow{\rho}\,\psi_\lambda(\overrightarrow{\rho})\delta V^{2D}(\rho)\psi_\lambda(\overrightarrow{\rho})$$
$$= \left[\frac{1}{(2\pi)^2}\right]^2 \int d^2\hat{p}\, d^2\hat{q}\,\psi_\lambda(\hat{p})V^{2D}(\hat{q})\psi_\lambda(|\hat{\mathbf{p}}-\hat{\mathbf{q}}|)\Theta(\hat{p}_F-\hat{q}) \qquad (5)$$

In further calculations we find the ground state energy E_{ex} of the Schrodinger equation:

$$-\frac{\nabla^2}{2\mu}\psi_\lambda(\overrightarrow{\rho}) + V^{2D}(\rho)\psi(\overrightarrow{\rho}) = E_{ex}\psi_{ex}(\overrightarrow{\rho}), \qquad (6)$$

where $V^{2D}(\rho)$ is the quasi-two dimension Coulomb potential taking into account the static screening. Additionally, we should calculate the phase-space filling correction according to Eq. (5).

2.1. Coulomb potential in a quasi-two-dimensional quantum well

The Coulomb and exchange interactions in a quantum well should be transformed to take into account the fact of the reduced dimensionality due to the confinement.

The effective Coulomb potential in the well depends on the thickness and shape of the quantum well and on the concentration of free electrons.

We find the effective Coulomb potential assuming that all the particles occupy their lowest confined state in a quantum well with infinitely high barriers. In this case the wave functions of all the particles can be characterized by the quantum well thickness L.

As the first step, we obtain an effective "quasi-2D" Coulomb potential without static screening $V_0^{2D}(\overrightarrow{\rho})$ (see Eq. (11) below) by using the Coulomb interaction in 3D systems as a starting point, similarly to Ref. [15]. The Coulomb Hamiltonian in a 3D system is

$$H_{Coul} = \frac{1}{2}\sum_{i,j,\sigma,\sigma'}\int d^3r_i d^3r_j V_{Coul}(\mathbf{r}_i-\mathbf{r}_j)|\psi_\sigma(\mathbf{r}_i)|^2|\psi_{\sigma'}(\mathbf{r}_j)|^2, \qquad (7)$$

where σ denotes the spin quantum number, and

$$V_{Coul}(\mathbf{r}_1-\mathbf{r}_2) = \pm\frac{1}{(2\pi)^3}\int d^3q\frac{4\pi e^2}{\varepsilon q^2}\exp(i\mathbf{q}(\mathbf{r}_1-\mathbf{r}_2)), \qquad (8)$$

where ε is the static dielectric constant, and the $\mathbf{r}_i$, $i=1,2$ are the radius-vectors of the two interacting particles. We may express the $\mathbf{r}_i$ as coordinates in an arbitrary plane and perpendicular to this plane $\mathbf{r_i} \to (\overrightarrow{\rho_i}, z)$ and, similarly, components of the wave-vector $\mathbf{q}$ in the reciprocal space are $\hat{\mathbf{q}}$ and q_z. The signs $\pm$ are related to the electron–electron and electron–valence band hole interactions respectively. In writing Eq. (7) and below, we are using CGS units.

We exclude the 3D motion in the perpendicular direction by calculating the matrix elements of exponentials with wave-functions $\psi(z) = \sqrt{2/L}\cos(\pi z/L)$ assuming that the wave functions of the exciton and conduction electron–conduction hole pairs are completely confined within the quantum well of thickness L restricted by infinite barriers. The Coulomb vertex contains the product of two matrix elements having the form:

$$M_{z,z} = [\exp(izq_z)]_{\psi(z),\psi(z)} = \prod_{k=2}^{\infty}[1-(q_zL)^2/(2\pi k)^2]. \qquad (9)$$

The integral over q_z

$$\int_0^\infty \frac{dq_z}{2\pi}\frac{4\pi e^2[M_{z,z}(q_z)]^2}{\varepsilon[\hat{q}^2+q_z^2]} \qquad (10)$$

can be calculated numerically or represented with good accuracy by the function $[(4e^2/\varepsilon\hat{q})\arctan\tilde{q}_L/\hat{q}]$ where $\tilde{q}_L = 2\pi/\tilde{L}$ and

$$\frac{L}{\tilde{L}} = \int_0^\infty \frac{Ldq_z}{2\pi}[M_{z,z}(Lq_z/2\pi)]^2 \simeq 0.75.$$

As a result we can present the effective quasi-2D Coulomb interaction without screening as

$$V_0^{2D}(\hat{q}) = \frac{4e^2}{\varepsilon \hat{q}} \arctan \frac{\tilde{q}_L}{\hat{q}}. \tag{11}$$

The screened effective Coulomb potential in the random phase approximation has the form:

$$V^{2D}(\hat{q}) = \frac{4e^2 \arctan \frac{\tilde{q}_L}{\hat{q}}}{\hat{q} \varepsilon(\hat{q}, 0)} \tag{12}$$

where $\varepsilon(\hat{q}, 0)$ is the real part of the dielectric function that takes into account free electrons

$$\varepsilon(\hat{q}, 0) = \varepsilon \left[1 - \frac{4e^2}{\varepsilon \hat{q}} \arctan \frac{\tilde{q}_L}{\hat{q}} Re\chi(\hat{q}, 0) \right] \tag{13}$$

In the limit $\omega \rightarrow 0$ the real part of the dielectric susceptibility can be presented as

$$Re\chi(\hat{q}, 0) = -\frac{m^*}{\pi \hbar^2} \left\{ 1 - \Theta(\hat{q} - 2\hat{p}_F) \sqrt{1 - (2\hat{p}_F/\hat{q})^2} \right\} \tag{14}$$

And, finally, the screened effective Coulomb potential in the random phase approximation is

$$V^{2D}(\hat{q}) = \frac{4e^2 \arctan \frac{\tilde{q}_L}{\hat{q}}}{\hat{q}}$$
$$\times \left\{ 1 + \frac{4}{\pi \hat{q} a_0} \arctan \frac{\hat{q}_L}{\hat{q}} \left\{ 1 - \Theta(\hat{q} - 2\hat{p}_F) \sqrt{1 - (2\hat{p}_F/\hat{q})^2} \right\} \right\}^{-1}, \tag{15}$$

where $a_0 = \hbar^2 \varepsilon / m^* e^2$ is the radius of the 3D donor state.

Screening in quasi-2D systems was considered in early publications by using perturbation theory [3]. However, new experimental data [6,9] were interpreted as showing that the exciton binding energy decreases very sharply with an increase in the concentration of two-dimensional electrons for CdTe quantum wells and for GaAs/AlGaAs quantum wells [10].

We have calculated the absolute value of the exciton binding energy as a function of free electron concentration in the random phase approximation for 10 nm thick CdTe quantum wells, of the type studied experimentally in Refs. [6–9], assuming infinite-height barriers. The result is presented as curve 1 in Fig. 1(a). The phase-space filling correction of Eq. (5) is given in Fig. 1(a) by curve 2. The parameters used in our calculations are presented in Table 1.

An effective Rydberg energy of $E_B = 18$ meV for electron concentration of about 10^{10} cm^{-2} was estimated by Teran et al. [9] from the energy distance between the ground and first excited exciton states observed in their PLE spectrum. Such a value of E_B is obtained in our calculation at 10^9 cm^{-2} by using the parameters presented in Table 1. We calculate the quasi-2D Rydberg at zero concentration to be 22 meV. This is twice the 3D value of 11 meV. The relatively strong decrease of the effective Rydberg in the low concentration range from 0 to 10^9 cm^{-2} is explained by the strong screening of the Coulomb potential at $\hat{q} \leq 1/a_0$ in the random phase approximation as follows from Eq. (15).

From concentrations about 10^{10} cm^{-2}, the phase-space filling correction significantly decreases the binding energy. Extrapolating curve 2 up to the point where it crosses curve 1 in Fig. 1(a), we can estimate the electron concentration ($\simeq 3 \times 10^{11}$ cm^{-2}) above which the bound exciton states should disappear.

The decrease of the exciton binding energy due to screening and phase-filling correction is followed by decrease of its oscillator strength. At zero electron concentration the exciton oscillator strength is proportional to $[\int d^2\hat{q}/(2\pi)^2 \psi_{ex}(\hat{q})]^2 = [\psi_{ex}(\rho=0)]^2 \sim 1/a_{ex}^2$ where a_{ex} is the effective exciton radius. For the oscillator
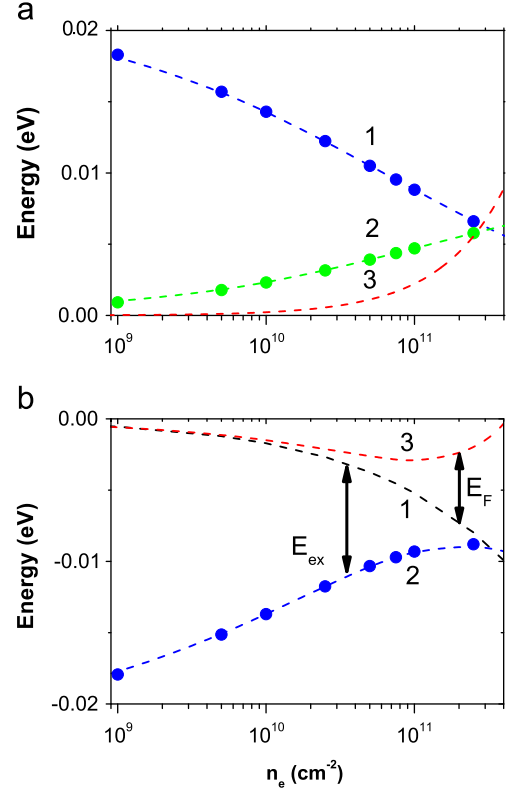
Fig. 1. (a) Curve 1 presents the dependence of the absolute value of the exciton binding energy on the free electron concentration for a 10 nm wide CdTe quantum well, taking into account only the static screening. Curve 2 presents the repulsive phase-space filling correction decreasing the exciton binding energy, and Curve 3 is the absolute value of the Fermi energy. (b) Curve 1 is the rigid shift of the band gap E_G corresponding to diagram (a) of Fig. 2. Curve 2 is the exciton binding energy with respect to E_G as a function of the electron concentration taking into account the static screening and phase-space filling effects. Curve 3 is the Fermi energy with respect to E_G.

Table 1
Parameters used in calculations: electron and hole effective masses, the binding energy of the 3D exciton in CdTe E_{ex}^{3D}, the quantum well thickness t_{QW}, the effective exciton radius a_B^{3D}, and the static dielectric constant ε.

m_e	m_h	E_{ex}^{3D} (meV)	t_{QW} (Å)	a_B^{3D} (Å)	ε
$0.107m_0$	$0.45m_0$	11.0	100	63	10.4

strength at finite electron concentration we have

$$A(n_e) = \left[\int \frac{d^2\hat{q} \Theta(\hat{q} - \hat{p}_F) \psi_{ex}(\hat{q})}{(2\pi)^2} \right] \psi_{ex}(\rho = 0). \tag{16}$$

In this case two mechanisms decrease the oscillator strength: the increase of the exciton radius and the phase-space filling restriction. The major effect is the increase of the exciton radius resulting from the decrease of the exciton binding energy. We should mention that some underestimation of the phase space filling at high electron concentrations occurs in our calculation of the exciton binding energy because we consider this effect as a perturbation only.

3. Hartree–Fock exchange corrections

We should say that the inelastic 2D plasmon interaction process due to Coulomb interaction with free electrons is significantly weaker for the electro-neutral exciton than for charged

particles. This process does not give a notable additional shift or broadening of the exciton line, in contrast to its effects for uncorrelated electrons and holes [16] or for the charged trion [15]. For the exciton, the cancellation of the electron and hole self-energy and vertex corrections leads to a decrease of this interaction. We will show that it is the Hartree–Fock exchange interaction that can describe the shift and broadening of the exciton band.

The early calculations of the band gap renormalization in quantum wells were done in Refs. [17–19].

It is convenient to illustrate the calculations of the exchange self-energy corrections by Feynman diagrams starting from the corrections to the single electron interacting with the Fermi sea of electrons neglecting the electron–valence-band hole exchange interaction for simplicity.

We consider the first order self-energy correction to the electron state due to Hartree–Fock exchange interaction, presented in Fig. 2(a), in the framework of the rigid shift approximation, taking the external wave vector equal to zero. This leads to a wavevector-independent shift of the conduction band and, therefore, of the exciton states.

The diagram illustrating the second order correction (Fig. 2(b)) can be obtained, for instance, from the Feynman diagrams in Fig. 37(b) of Ref. [20] by breaking one of the electron lines. Taking into account that we are interested in broadening of the exciton created by a $k \approx 0$ photon, we put the value of the wave-vector of the renormalized particle equal to zero. The correction to the exciton energy at zero wave-vector of the center of mass is given in Fig. 2(c). It can be seen that this diagram is obtained by putting the self-energy diagram of Fig. 2(b) at $\hat{Q}=0$ into the electron line of the exciton.

Finally, in order to describe the self-energy corrections to the exciton state, we have to sum the series of multiple scattering processes. In calculations of the exciton Green function we consider only the ground state. This allows us to transform the series into a geometrical progression. Therefore, the major part of the problem is to calculate the self-energy correction to the ground state.

3.1. The Hartree–Fock exchange interaction

First of all we have to express the exchange self-energy correction to the exciton through the 2D Coulomb-like $V(q)_{exch}^{2D}$ Hamiltonian taken in the form:

$$H_{exch} = \frac{1}{2}\sum_{i,j,\sigma \neq \sigma'} \int d^3r_i d^3r_j V_{exch}(\mathbf{r}_i - \mathbf{r}_j)\psi_\sigma(\mathbf{r}_i)\psi_\sigma(\mathbf{r}_j)^*\psi_{\sigma'}(\mathbf{r}_j)\psi_{\sigma'}(\mathbf{r}_i)^*,$$

(17)

where the diagram of Fig. 2(a) contains the vertex

$$V_{exch}(\mathbf{r}_1 - \mathbf{r}_2) = -\frac{1}{(2\pi)^3}\int d^3q \frac{4\pi e^2}{\varepsilon q^2}\exp(i\mathbf{q}(\mathbf{r}_1 - \mathbf{r}_2)).$$

(18)

The diagram of Fig. 2(c) contains the vertex depending on the wave-vector $\mathbf{q}$ and the similar vertex depending on $(\mathbf{p}+\mathbf{q})$.

The integrals over z_1 and z_2 for both diagrams we calculate similarly to Eqs. (9) and (10). Then the first integral over dq_z gives the same expression as Eq. (11).

3.1.1. Rigid shift of the conduction band
This leads to a rigid shift of the conduction band states δE_R

$$\delta E_R = \frac{1}{(2\pi)^2}\int d^2\hat{q}\frac{2e^2}{\varepsilon\hat{q}}\arctan\frac{\tilde{q}_L}{\hat{q}}.$$

(19)

Approximately, the dependence of this equation on the electron concentration is $\sqrt{n_e}$. The result of the numerical calculation of the band edge shift is presented in Fig. 1(b) by curve 1. The exciton
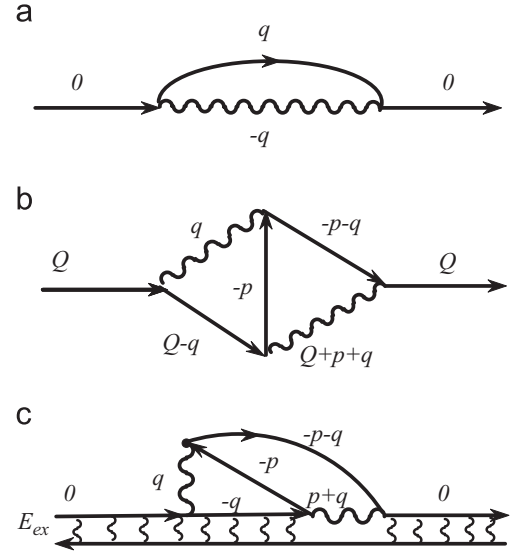
Fig. 2. (a) Feynman diagram which describes the rigid shift of the electron energies. (b) The second order exchange self-energy correction to the electron state. (c) The second order self-energy correction to the exciton state (double horizontal line connected by the wavy Coulomb lines) due to exchange interaction, obtained from diagram (b) at $Q=0$. Solid lines are the electron and hole Green functions, the wavy lines are the exchange vertexes.

binding energy with respect to the shifted band edge is presented in Fig. 1(b) by curve 2.

3.1.2. Shift and broadening of the exciton band due to the second order correction
The expression corresponding to the diagram of Fig. 2(c) contains two matrix elements over the internal wave function of the ground state exciton. The first of them has the form:

$$\mathcal{M}_{11}(\hat{q}) = \int d^2\rho|\psi_1(\rho)|^2\exp(i\hat{\mathbf{q}}\rho) = \left\{\frac{1}{[1+(\hat{q}a_B/2)^2]^{3/2}}\right\}$$

(20)

and a similar equation can be written for $\mathcal{M}_{11}(|\hat{\mathbf{q}}+\hat{\mathbf{p}}|)$.

The structure of the exchange loop in Fig. 2(c) $P_{\hat{q}}^{exch}(\hbar\omega)$ differs from the Coulomb contribution [15] and has the form:

$$P_{\hat{\mathbf{q}}}^{exch}(\hbar\omega) = \int \frac{d^2\hat{q}}{(2\pi)^2}\frac{4e^2}{\varepsilon\hat{q}}\arctan\frac{\tilde{q}_L}{\hat{q}}$$

$$\int_0^\infty \frac{dq_z^1}{2\pi}4\pi e^2 M_{zz}^2(q_z^1)\mathcal{P}_{\hat{\mathbf{q}},q_z^1}^{exch}(\hbar\omega),$$

(21)

where the variable $q_z^1 = (\mathbf{p}+\mathbf{q})_z$ is introduced. The function $\mathcal{P}_{\hat{\mathbf{q}},q_z^1}^{exch}(\hbar\omega)$ is

$$\mathcal{P}_{\hat{\mathbf{q}},q_z^1}^{exch}(\hbar\omega) = -\int \frac{d^2p}{2\pi}\frac{\mathcal{M}_{11}(\hat{q})\mathcal{M}_{11}(|\hat{\mathbf{q}}+\hat{\mathbf{p}}|)}{\varepsilon|\hat{\mathbf{q}}+\hat{\mathbf{p}}|^2+(q_z^1)^2}\eta(\mathbf{p},\mathbf{p}+\mathbf{q},\hbar\omega)$$

(22)

and

$$\eta(\hat{\mathbf{p}},\hat{\mathbf{p}}+\hat{\mathbf{q}},\hbar\omega) = \left\{\frac{1}{\hbar\omega+i\delta-\omega_{\hat{\mathbf{p}}\hat{\mathbf{q}}}} - \frac{1}{\hbar\omega+i\delta+\omega_{\hat{\mathbf{p}}\hat{\mathbf{q}}}}\right\}.$$

(23)

We have neglected the exciton kinetic energy in the final state (recoil effect) which is small compared to the energy of the electron–conduction hole pair.

The wave-vector dependence of both matrix elements $\mathcal{M}_{ex}(\hat{q})$ and $\mathcal{M}_{ex}(|\hat{\mathbf{q}}+\hat{\mathbf{p}}|)$ arises at values of the order of the reciprocal Bohr radius of the exciton $1/a_B^{2D}$. We will assume this quantity to be essentially larger than the Fermi wave-vector p_F which is the characteristic value for $\hat{\mathbf{p}}$. Therefore, we approximate the product
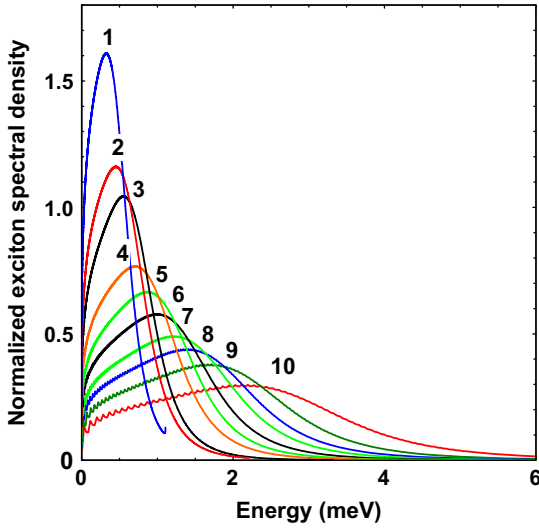
Fig. 3. Broadening and shift of the normalized to unity, spectral density of the exciton ground state caused by the second order exchange interaction for ten electron concentrations in a 10 nm CdTe/CdMgTe quantum well. The zero of energy corresponds to the exciton ground state at zero temperature and zero electron concentration. The ten electron concentrations expressed in 10^{10} cm^{-2} are equal to 0.5, 1.0, 1.5, 2.5, 3.75, 5.0, 7.5, 10.0, 15.0, and 25.0.

Fig. 4. Spectral density of the exciton ground state for a 10 nm CdTe/CdMgTe quantum well parameters at increasing electron concentration. The zero of energy corresponds to the exciton ground state at zero temperature and electron concentration equal to 0.5×10^{10} cm^{-2}. As compared to Fig. 3, the threshold energy of each exciton band is shifted upwards: Here, in addition to the second order shift and broadening due to exchange interaction, the static screening, the first-order rigid shift due to exchange interaction, the phase-space filling effect, and the decrease of the oscillator strength are all taken into account. The ten electron concentrations expressed in units of 10^{10} cm^{-2} are equal to 0.5, 1.0, 1.5, 2.5, 3.75, 5.0, 7.5, 10.0, 15.0, and 25.0.

of these matrix elements by the expression $\mathcal{M}_{ex}(\hat{q})\mathcal{M}_{ex}\,(|\hat{\mathbf{q}}+\hat{\mathbf{p}}|) \approx \mathcal{M}_{ex}(\hat{q})^2$. Taking into account that the integral over dq_z^1 is restricted by $q_z^1 \approx q_L = 2\pi/L$ we take the function $\mathcal{P}_{\hat{q},q_z^1}^{exch}(\hbar\omega)$ out of the integral of Eq. (24) at $q_z^1 = q_L$. After these simplifications the integral over dq_z^1 gives $\tilde{L}^{-1}$ and the remaining integral over d^2p in Eq. (22) can be calculated analytically.

Finally, we obtain the exciton self-energy correction due to exchange interaction in the form:

$$\delta E_{ex}(\hbar\omega) = \frac{1}{(2\pi)^2}\int d^2\hat{q}\left[\frac{4e^2\mathcal{M}_{ex}(\hat{q})^2}{\varepsilon\hat{q}}\arctan\frac{\tilde{q}_L}{\hat{q}}\right]$$
$$\times \int d^2\hat{p}\frac{e^2}{\varepsilon\tilde{L}[|\hat{\mathbf{q}}+\hat{\mathbf{p}}|^2+(q_L)^2]}\eta(\hat{\mathbf{p}},\hat{\mathbf{p}}+\hat{\mathbf{q}},\hbar\omega). \quad (24)$$

The broadening of the exciton absorption band and the upward shift of its peak with respect to the exciton line at zero electron concentration, resulting from this correction, are shown in Fig. 3 for a set of ten electron concentrations ranging up to $n_e = 2.5 \times 10^{11}$ cm^{-2}. The absorption curves have the form:
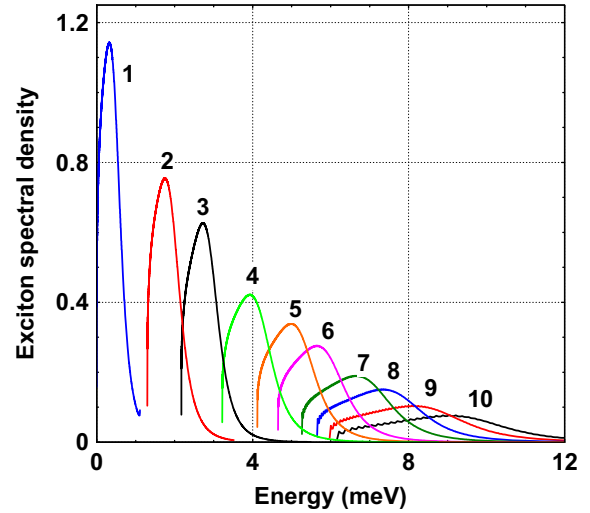
$$\alpha(\omega) \sim \frac{\Gamma(\omega)}{(\hbar\omega - E_{ex}(n_e=0) - \Delta(\omega))^2 + \Gamma^2(\omega)}, \quad (25)$$

where $\Gamma(\omega)$ and $\Delta(\omega)$ are the imaginary and real parts of the exciton self-energy correction of Eq. (24). For convenience the absorption band profiles are normalized to unity in Fig. 3. We see that the values of the upward shifts are comparable with the effect of the rigid downward shift due to the first order exchange interaction in Fig. 1(b).

In Fig. 4 we present the transformed spectra of Fig. 3 after the first-order rigid shift due to exchange interaction, the phase-space filling effect, as well as the decrease of the oscillator strength are all taken into account. The shape of the exciton absorption band can be represented in this case as

$$\alpha(\omega) = 2A(n_e)\frac{\Gamma(\omega)}{(\hbar\omega - E_{ex}(n_e) - \Delta(\omega))^2 + \Gamma^2(\omega)}, \quad (26)$$

where $A(n_e)$ is given by Eq. (16). The position of the exciton ground state at zero temperature and electron concentration equal to 0.5×10^{10} cm^{-2} is taken as the point of reference.

The parameters used in our calculations are presented in Table 1.

4. Comparison with experimental data

We have compared the above theory with optical absorption data at 2 K for a 10 nm CdTe/CdMgTe single quantum well at zero magnetic field. This sample was grown by Molecular Beam epitaxy on a CdTe$_{0.88}$Zn$_{0.12}$Te substrate. The alloy substrate is transparent to about 1640 meV, allowing direct measurements of the optical transmission spectrum in the energy region (1610–1630 meV) of the heavy-hole exciton in the CdTe quantum well. Also, the substrate imposes a large biaxial strain on the CdTe well layer, splitting off light-hole transitions to high energies, which simplifies the optical spectrum. The upper CdMgTe barrier was doped with donors so as to give $n_e = 1.5 \times 10^{11}$ cm^{-2} in the well in equilibrium [21].

Optical data for this sample were provided by Ronald Cox of Néel Institute. During the optical transmission measurements, done using a tungsten lamp source, the electron concentration could be varied down to a low value by pumping the sample with blue laser light. The precise dependence of n_e on pumping light intensity was not known but the minimum concentration was estimated to be in the range $(0.2-0.4) \times 10^{11}$ cm^{-2} as judged from the intensity of the X^- (trion) resonance.

For comparison with this experimental data we will use spectra of Fig. 4 fitting the absolute exciton energy. Results are presented in Fig. 5. As it is seen, the shift of the exciton maximum agrees well with experimental data if we take the electron concentration for the lowest band equal to 1.5×10^{10} cm^{-2} and for the highest one to 1.5×10^{11} cm^{-2}. The lowest value appears to be slightly less than the value estimated in experiment $(2-4 \times 10^{10}$ cm$^{-2})$ while the upper value agrees well with experimental data.

However, the experimental broadening values exceed notably the calculated values for all the samples. This may be attributed to the existence of some additional broadening mechanism which was not taken into account in our calculations.
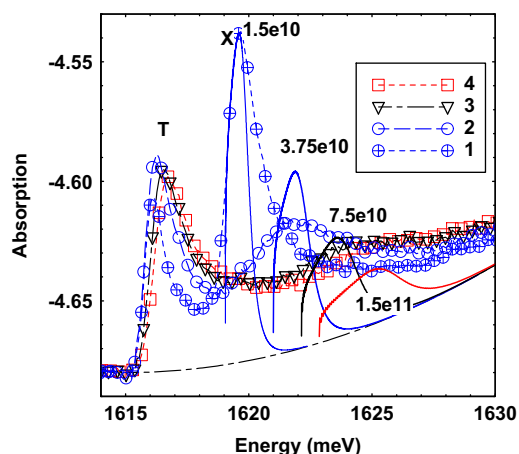
Fig. 5. Curves 1–4 are the experimental data on absorption of a 10 nm CdTe (0.3% Mn) single quantum well in zero magnetic field at different free electron concentrations. A resonance peak (*T*) corresponds to creation of the singlet trion appearing below the exciton resonance (*X*). Solid curves are the calculated exciton line profiles at free electron densities of 1.5, 3.75, 7.5, and 15.0 in 10^{10} cm^{-2}. The dashed curve is a background added to the calculated spectra.

The existence of an additional mechanism of exciton state decay might be assumed because the ground exciton state is not the lowest bound state in the presence of the Fermi sea. At least the trion state might serve as such a state. Another reason for the deviation could be the forced simplifications admitted in our calculations.

5. Conclusion

The shift and broadening of the exciton absorption bands in CdTe/CdMgTe quantum wells as a function of the free carrier concentration at zero magnetic field is investigated. It is shown that the exciton's shift and broadening behavior is related to the Hartree–Fock exchange interaction between the electron bound to the valence band hole and the free carriers. This is in contrast to the case of the charged trion, where it is the Coulomb interaction with the free electrons that plays the leading role. The calculations

performed have shown that reasonable agreement can be obtained with experimental data.

References

[1] G.D. Mahan, Phys. Rev. 153 (1967) 882.
[2] S. Schmitt-Rink, C. Ell, H. Haug, Phys. Rev. B 33 (1986) 1183.
[3] S. Schmitt-Rink, D.S. Chemla, D.A.B. Miller, Adv. Phys. 38 (1989) 89.
[4] P. Hawrylak, Phys. Rev. B 44 (1991) 3821.
[5] G.E.W. Bauer, Phys. Rev. B 45 (1992) 9153.
[6] V. Huard, R.T. Cox, K. Saminadayar, A. Arnoult, S. Tatarenko, Phys. Rev. Lett. 84 (2000) 187.
[7] R.T. Cox, V. Huard, C. Bourgognon, K. Saminadayar, S. Tatarenko, R.B. Miller, Acta Phys. Pol. A 106 (2004) 287.
[8] R.T. Cox, R.B. Miller, K. Saminadayar, T. Baron, Phys. Rev. B 69 (2004) 235303.
[9] F.J. Teran, Y. Chen, M. Potemski, T. Wojtowicz, G. Karczewski, Phys. Rev. B 73 (2006) 115336.
[10] S.I. Gubarev, O.V. Volkov, V.A. Koval'skii, D.V. Kulakovskii, I.V. Kukushkin, JETP Lett. 76 (2002) 575.
[11] M. Combescot, O. Betbeder-Matibet, M.A. Dupertuis, Solid State Commun. 147 (2008) 474.
[12] M. Combescot, O. Betbeder-Matibet, F. Dubin, Eur. Phys. J. B 42 (2004) 63.
[13] M. Combescot, O. Betbeder-Matibet, Solid State Commun. 126 (2003) 687.
[14] Shiue-Yuan Shiau, Monique Combescot, Yia-Chung Chang1, Phys. Rev. B 86 (2012) 115210.
[15] A.A. Klochikhin, V.P. Kochereshko, L. Besombes, G. Karczewski, T. Wojtowicz, J. Kossut, Phys. Rev. B 83 (2011) 23.
[16] S. Schmitt-Rink, C. Ell, S.W. Koch, H.E. Schmidt, H. Haug, Solid State Commun. 52 (1984) 123.
[17] D.A. Kleinmann, R.C. Miller, Phys. Rev. B 32 (1985) 2266.
[18] S. Das Sarma, R. Jalabert, S.-R. Eric Yang, Phys. Rev. B 41 (1990) 8288.
[19] Gerrit E. Bauer, Tsuneya Ando, J. Phys. C: Solid State Phys. 19 (1986) 1537.
[20] D. Pines, P. Nozieres, The theory of quantum liquids, in: Normal Fermi Liquids, vol. 1, W.A. Benjamin, Inc. NY, Amsterdam, 1966.
[21] This CdTe well was doped with 0.3%Mn, for studying electron spin-polarization effects in magnetic field. This was of no concern for the present analysis of zero field spectra: the very low concentration of Mn does not significantly broaden the exciton resonance.